Solid-State NMR Investigations of Poly[(acrylonitrile)-rotaxa-(60-crown-20)]

K. Nagapudi, J. Leisen, and H. W. Beckham*

Polymer Education and Research Center, School of Textile and Fiber Engineering, Georgia Institute of Technology, Atlanta, Georgia 30332-0295

H. W. Gibson

Department of Chemistry, Virginia Polytechnic Institute & State University, Blacksburg, Virginia 24061

Received August 18, 1998

ABSTRACT: Solid-state NMR has been used to investigate the structure, dynamics, and morphology of the polyrotaxane prepared by polymerizing acrylonitrile in the presence of 60-crown-20. For solid poly-[(acrylonitrile)$_n$-rotaxa-(60-crown-20)$_x$] with $x/n = 0.01$, the 60-crown-20 was found to be phase-separated, amorphous, and highly mobile at room temperature. 2D WISE NMR revealed the presence of less mobile crown segments that were attributed to those in contact with the rigid PAN phase at the interfacial regions. Compared to unthreaded PAN, the T_g of the host backbone was slightly depressed (90 °C vs 110 °C), as measured by solid-state ^{1}H NMR. These PAN T_g values were undetectable with DSC. Dipolar magnetization transfer (i.e., spin diffusion) experiments on the polyrotaxane revealed typical smallest diameters of 6−8 nm for the 60-crown-20 domains and NMR long periods of 20−26 nm. The long periods were compared with electron density correlation lengths computed from SAXS data. Upon heating the polyrotaxane to 80 °C, the primary change in the domain structure was a reduction in the size of the interface. A physical blend of PAN and 60c20 was also found to be phase separated, with a sharper interface than the polyrotaxane.

Introduction

Polyrotaxanes are linear polymers onto which cyclic molecules are threaded. Synthetic routes have been developed, and a wide variety of these materials have been reported.[1,2] Much of this work is apparently driven by the known influence of molecular topology and dynamics on bulk physical properties. In polyrotaxanes, solubilities and melting/softening temperatures,[3−5] and therefore processabilities, are modified by threading. Morphologies and chain mobilities, and therefore mechanical and transport properties, can be significantly altered by threading. While some studies of polyrotaxane morphologies have appeared,[6−9] very little is known about mechanical[10] or transport properties.

It has been noted that polyrotaxanes can exhibit properties that are different from those of the unthreaded backbone, analogous copolymers, or analogous blends. The difference arises from the ability to incorporate permanent structure-modifying components that remain mobile with respect to the polymer backbone. While structure-dependent properties can be modified by incorporation of new components via copolymerization, high localized mobility cannot be retained since the structure-modifying component is tied up in the backbone as one of the comonomers. Molecular-mobility-dependent properties may be modified by blending with highly mobile low-molecular-weight components, but immiscibility or leaching out of the additive often precludes the production of stable blends. Of course, introduction of structural modifications and localized mobility can be achieved by copolymerization with monomers containing flexible side groups. Compared to these materials, main-chain polyrotaxanes comprised of flexible macrocycles are structurally similar, except the flexible side groups (i.e., macrocycles) are not restricted to defined spacings along the host backbone.

Our work in this area is focused not only on synthesizing new polyrotaxanes but also on fully characterizing their molecular dynamics, morphology, and bulk physical properties. For example, we have synthesized some new polyurethane rotaxanes and conducted dynamic mechanical measurements[11] in conjunction with solid-state NMR measurements to identify the molecular origin of the dynamic mechanical loss processes. One of the polyurethane/crown ether rotaxanes clearly exhibited new localized motions (compared to the unthreaded backbone) as evidenced by new peaks in the loss tangent versus temperature curves.[12] Thus, polyrotaxanation may be a new route to plasticization or toughening of polymers, both of which depend on the existence of localized molecular motions.

In this report, we present results on the structure and mobility of the polyrotaxane produced by polymerizing acrylonitrile in the presence of 60-crown-20. Poly-[(acrylonitrile)-rotaxa-(60-crown-20)], PAN-rotaxa-60c20, was prepared via traditional free-radical polymerization initiated with AIBN in the presence of a large concentration of the macrocycle.[13] A series of consecutive dissolution steps followed by precipitation in good solvents for the crown removed the unthreaded cyclics to give the polyrotaxane.[1] For sufficiently high crown loadings (>25 mass %), the polyacrylonitrile−rotaxane was soluble in methanol and exhibited modified thermal properties when compared with those of the unthreaded backbone. For example, differential scanning calorimetry revealed transitions at −65 and at 55 °C which roughly correspond to the glass and melting transitions, respectively, for the free 60-crown-20.[13] The following

* Author to whom correspondence should be addressed.

10.1021/ma9813082 CCC: $18.00
Published on Web 04/09/1999

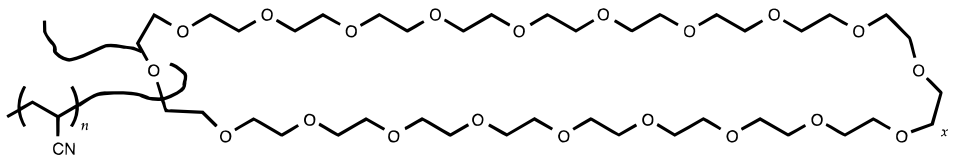

Figure 1. Structure of poly[(acrylonitrile)$_n$-rotaxa-(60-crown-20)$_x$], or PAN-rotaxa-60c20. The 60-crown-20 is shown in its most extended form, about 3.6 nm from end to end; this form has no cavity and can therefore not accommodate a threaded polymer chain. The actual maximum distance between PAN segments and 60c20 segments is therefore less than 3.6 nm.

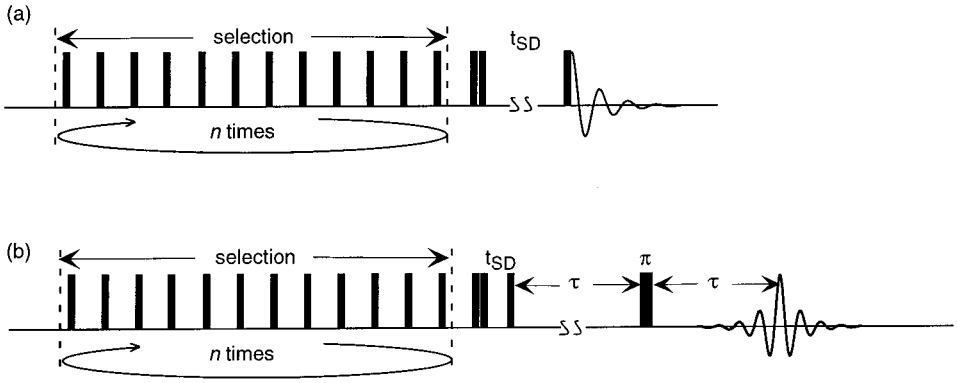

Figure 2. Timing diagrams for pulse sequences used to measure (a) spin diffusion following selection of mobile-phase magnetization with a dipolar filter and (b) mobile-phase T_2 values using a Hahn echo sequence after the dipolar filter (t_{SD} = 10 μs while τ was varied).

report details some ^{1}H and ^{13}C solid-state NMR studies on the structure, dynamics, and morphology of poly-[(acrylonitrile)$_n$-rotaxa-(60-crown-20)$_x$] with $x/n = 0.01$.

Experimental Section

The free 60-crown-20 (60c20) sample was prepared according to published synthetic methods.[14] The structure of the PAN-rotaxa-60c20 system is shown in Figure 1. Details of the synthesis have been provided.[13] The sample used in this study was characterized by ^{1}H NMR spectroscopy as a solution in DMSO-d_6 on a Bruker DRX-500 spectrometer. A recycle delay of 20 s was used to ensure quantitative analysis. The 60c20 threading level (x/n) was determined to be 0.01, which corresponds to 15% crown by mass.[15]

A physical blend of PAN and 60c20 was prepared by dissolving both components in dimethylformamide and then precipitating in hexane. From ^{1}H NMR spectroscopy in DMSO-d_6, the molar ratio of 60c20 to PAN repeat units is 0.025. Both the blend and the polyrotaxane were vacuum-dried at 80 °C for 3 days or until no more changes were observed in their solid-state ^{1}H NMR line shapes. Differential scanning calorimetry was conducted at 5 °C/min on a Setaram TG-DSC 111 under a nitrogen purge of approximately 30 mL/min.

All solid-state NMR measurements were carried out on a Bruker DSX-300 spectrometer in a Bruker double-resonance MAS probehead. Standard cross-polarization (CP) and direct-polarization (DP) (i.e., single-pulse excitation) pulse techniques were used with ^{1}H and ^{13}C 90° pulses of 4 μs. Unless stated otherwise, recycle delays of 3 s and sample spinning speeds of 5 kHz were employed. A TOSS (total suppression of spinning sidebands) sequence[16] was used in the case of the polyrotaxane to provide a spectrum bereft of spinning sidebands. For ^{13}C spectra, 4K to 10K scans were accumulated for signal averaging. Two-dimensional wide-line separation (2D WISE) spectra[17,18] were collected with a contact time of 250 μs and a recycle delay of 3 s; 84 t_1 increments of 4 μs were measured for spectral widths of 125 kHz in the ^{1}H dimension. All other relevant spectral acquisition parameters are provided in the figures and associated captions.

^{1}H dipolar magnetization transfer (i.e., spin diffusion) experiments were conducted in the static mode (i.e., without magic-angle sample spinning). Recycle delays of 5 s, ^{1}H 90° pulse lengths of 4 μs, and ^{1}H 180° pulse lengths of 8 μs were used. The timing diagram for the spin diffusion pulse sequence is shown in Figure 2a. A dipolar filter selection sequence[19] consisting of 12 90° pulses separated by 15 μs delays was employed for 16 consecutive loops to establish the initial magnetization gradient; the mobile-phase magnetization was selected and then allowed to spin diffuse to the rigid phase. The variable spin diffusion time (t_{SD}) was incremented from 1 μs to 800 ms. Following the spin diffusion period, the magnetization was detected as a free induction decay (FID). For ^{1}H spectra, 32 scans were collected for each spin diffusion time. To correct for spin−lattice relaxation during the spin diffusion time, the experiment was conducted a second time but with the selection filter removed (number of dipolar filter cycles, n = 0). After normalization to $I_{cr}(0)$, the spectral intensity corresponding to the crown, the ratio of I_{cr}(with selection) to I_{cr}(without selection) provided the spin diffusion data as a function of t_{SD}.

To examine the structure of the material selected with the dipolar filter, cross-polarization to ^{13}C was added just after the selection sequence shown in Figure 2a. This experiment was conducted while magic-angle spinning at 6 kHz, using a t_{SD} = 10 μs, a 1 ms CP time, and a 3 s recycle delay. The ^{13}C FID was detected with ^{1}H decoupling.

The spin diffusion coefficient for the mobile phase was computed from the average T_2 of the selected mobile-phase magnetization. This was measured using the pulse sequence shown in Figure 2b by placing a Hahn echo sequence directly after the selection filter. For these measurements, t_{SD} was fixed at 10 μs and τ was incremented from 20 μs to 3 ms. After normalization, the echo maxima were plotted as a function of 2τ to provide the echo decay curves.

Results and Discussion

Figure 3 shows the ^{13}C solid-state NMR spectra for 60-crown-20[14] at room temperature. The spectrum at the bottom is the conventional CP/MAS spectrum measured with a contact time of 2 ms. While the ^{13}C NMR spectrum of 60c20 in solution contains one primary peak, the solid-state spectrum contains two major peaks at 70.8 and 72.3 ppm. (The low-intensity peak at 62 ppm is due to end-group carbon residues that remained as linear byproduct impurities from the crown synthesis.) Attributed to different conformations of the ethyleneoxy segments, the two major peaks have been

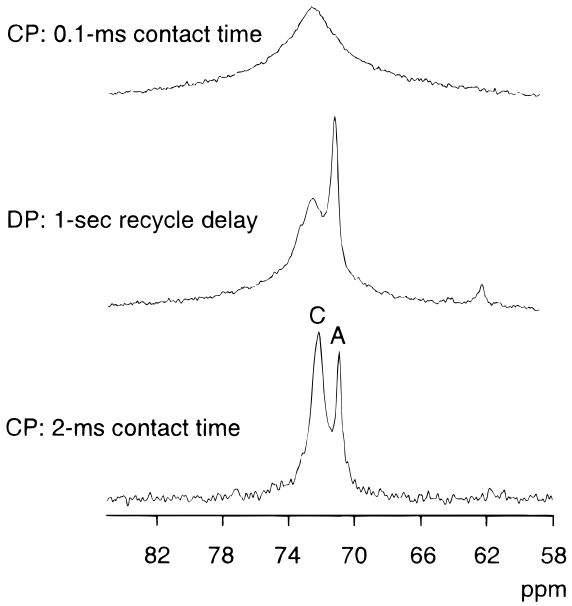

Figure 3. ^{13}C solid-state NMR spectra of 60-crown-20 measured with magic angle spinning at room temperature. C = crystalline, A = amorphous.

assigned using simple spectral editing techniques as described in Figure 3. The middle spectrum in Figure 3 is the single-pulse excitation (DP) spectrum collected with a recycle delay of 1 s. The major peak here appears at 70.8 ppm and is assigned to the conformers of the amorphous phase. The top spectrum of Figure 3 is a CP/MAS spectrum collected with a short contact time of 100 μs to discriminate for the more rigid conformers. The major peak here appears at 72.3 ppm, which is assigned to the conformers typical of the crystalline region. These assignments are supported by spectra at elevated temperatures, in which the upfield peak (70.8 ppm) increases in intensity as the temperature is increased. Note the crystalline peak is broader than the amorphous peak; this agrees with data reported in the literature for poly(ethylene oxide) (PEO) and is attributed to inefficient decoupling due to interfering backbone motions on the same time scale (i.e., $\tau_c \approx \omega_1^{-1}$).[20] DP spectra measured as a function of recycle delay reveal an increase in the relative intensity of the downfield peak (72.3 ppm) with increasing recycle delay, further confirming its relation to the crystalline regions.

Figure 4 shows the ^{13}C DP/MAS and CP/MAS/TOSS spectra of the PAN-rotaxa-60c20 and the ^{13}C CP/MAS spectra of the unthreaded PAN backbone and a physical blend of PAN and 60-crown-20. The CP/MAS/TOSS spectrum of the polyrotaxane contains well-resolved resonances for the backbone (28−42 ppm, overlapping methylene and methine), the side-chain nitrile (115−127 ppm), and the incorporated crown ether (66−75 ppm). Close inspection of the crown region in the CP spectrum of the PAN-rotaxa-60c20 reveals a prominent resonance at ∼71 ppm and a small shoulder at ∼72.5 ppm. By comparison with the 60-crown-20 spectra of Figure 3, it is concluded the crown is predominantly amorphous when threaded onto the linear polymer. Spectra taken at T = 70 °C, that is above the melt temperature of the free 60c20, still contain the small shoulder at ∼72.5 ppm, thus proving it is not due to the presence of a small fraction of 60c20 crystalline units in the polyrotaxane. The DP spectrum measured with 1 s recycle delay proves the 60-crown-20 is also highly

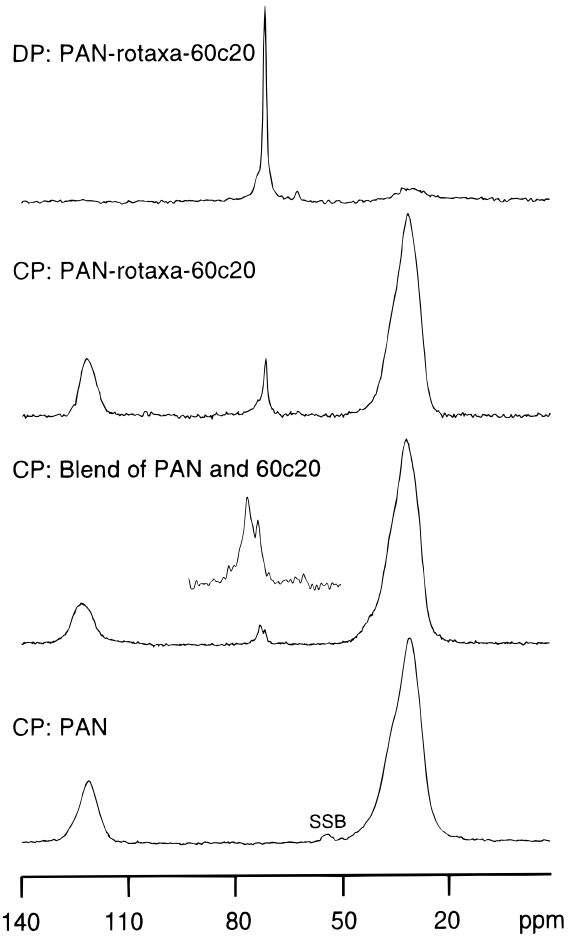

Figure 4. ^{13}C solid-state NMR spectra of PAN-rotaxa-60c20, a solution-blended mixture of PAN and 60c20, and the unthreaded PAN backbone. The crown region of the blend spectrum is also shown expanded. Temperature = 25 °C. Contact time for CP spectra = 2 ms. SSB = spinning sideband.

mobile in the polyrotaxane. The ^{13}C CP/MAS spectrum of the physical blend appears to be a simple superposition of the CP/MAS spectrum of PAN with the CP/MAS spectrum of 60c20 (Figure 3). The crown region is expanded just above this spectrum to more clearly show the similarity with the CP/MAS spectrum of the free 60-crown-20. Since the 60c20 is behaving like free 60c20, a phase-separated system is suggested for the physical blend.

The ^{13}C CP and DP spectra in Figure 4 clearly reflect the high mobility of the incorporated 60-crown-20 compared to that of the PAN backbone. More detailed information on molecular structure and dynamics is provided by 2D WISE NMR which correlates the ^{13}C NMR structural data with the dynamical content of solid-state ^{1}H NMR line shapes. At room temperature, the ^{1}H NMR line shape of PAN-rotaxa-60c20 consists of a narrow component superimposed on a broad component (see Figure 7, without selection). If the material is phase separated, the narrow component ($\Delta\nu_{1/2} \approx 600$ Hz) is due to the 60-crown-20 and the broad component ($\Delta\nu_{1/2} \approx 60$ kHz) is due to the PAN, since this measurement temperature lies above the 60c20 T_g (−65 °C) and below the PAN T_g (92−110 °C). The 2D WISE spectra of PAN-rotaxa-60c20 and PAN are shown in Figure 6 and reveal the polyrotaxane is phase separated. A narrow ^{1}H line shape component ($\Delta\nu_{1/2} \approx 600$ Hz) is observed only for the crown ether resonance (∼71 ppm on the ^{13}C axis). The ^{1}H line shapes corresponding to

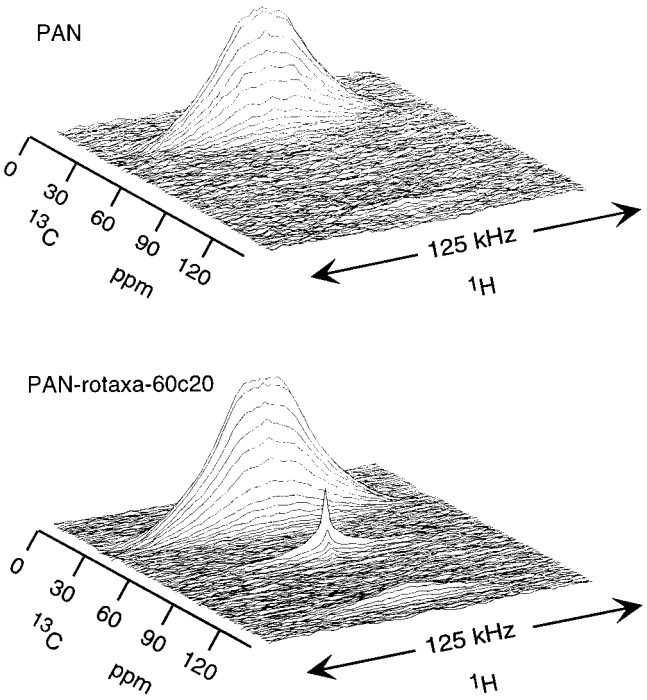

Figure 5. 2D WISE spectra of PAN and PAN-rotaxa-60c20 at 25 °C. The ^{1}H line widths for the PAN backbone are nearly equivalent in both spectra. The 60c20 ^{1}H line shape in the PAN-rotaxa-60c20 spectrum (~71 ppm on the ^{13}C axis) could be clearly deconvoluted into two components of different widths. This indicates that the crown consists of both mobile and less mobile segments in the polyrotaxane. The less mobile segments are attributed to those in contact with the rigid PAN. The bicomponent 60c20 ^{1}H line shape does not faithfully represent the component mass fractions due to the short contact time employed (250 μs) which discriminates against highly mobile segments.

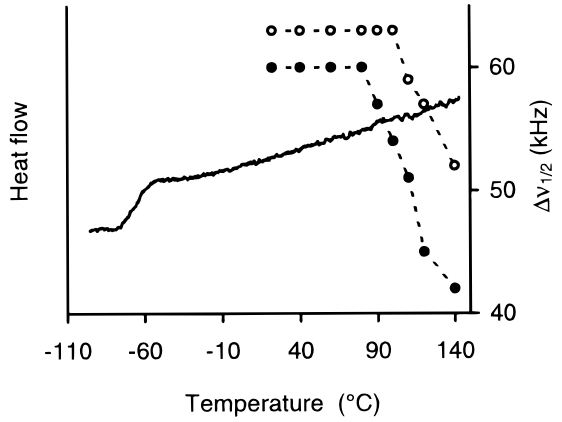

Figure 6. DSC thermogram of PAN-rotaxa-60c20 (solid line) and broad-component line width from the solid-state ^{1}H NMR spectrum (dashed line) of PAN-rotaxa-60c20 (●) and PAN (○). The 60c20 T_g is seen at −64 °C in the DSC trace. The T_g of PAN is not detected by DSC but is clearly seen by solid-state NMR as the temperature at which the ^{1}H line width begins to decrease. This temperature is 110 °C for the unthreaded PAN backbone (○) and 90 °C for the PAN backbone in PAN-rotaxa-60c20 (●).

the PAN backbone centered around 30 ppm and the nitrile group at ~123 ppm are much broader ($\Delta\nu_{1/2} \approx$ 60 kHz) and thereby reflect the immobility of the linear PAN backbone at room temperature. These line widths are similar for the unthreaded PAN backbone ($\Delta\nu_{1/2} \approx$ 63 kHz), thus providing no evidence for significant mixing of the crown and PAN in the polyrotaxane. A

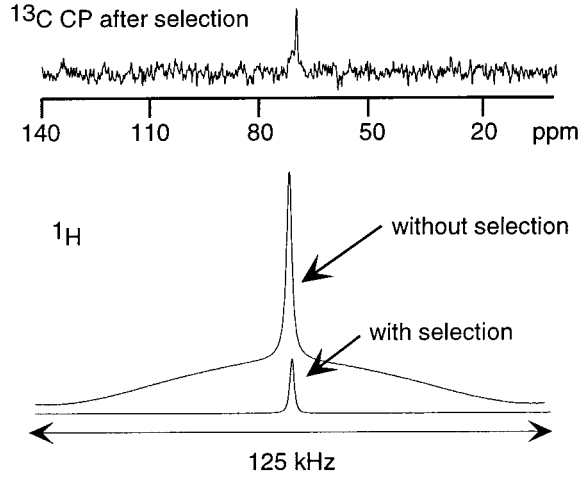

Figure 7. Static-mode solid-state ^{1}H NMR spectrum of PAN-rotaxa-60c20 measured with and without selection of the mobile-phase magnetization using a dipolar filter. Following selection, the magnetization was cross-polarized to the carbons and measured under MAS and ^{1}H decoupling. The ^{13}C CP/MAS spectrum shown at the top reveals the selected magnetization is due to the 60c20 segments only.

two-component ^{1}H line shape is observed for the crown, signifying more than one type of dynamic environment for the threaded 60c20. Crystalline 60c20 units in the polyrotaxane were ruled out by measuring the 2D WISE spectrum at 70 °C which is above the crown T_m; a two-component ^{1}H line shape was observed at this temperature also. The more rigid crown units are attributed to those in intimate contact with the rigid PAN phase.

Thus, incorporating 60-crown-20 onto the PAN backbone does not significantly change the backbone mobility at room temperature, even though the crown is present as a 15% mass fraction, amorphous, and highly mobile since room temperature is about 90 °C above the T_g of the free 60c20. These results are not surprising for a phase-separated material in which the crown does not plasticize the PAN. It is interesting that the crown remains amorphous in such a phase-separated system; threaded macrocycles have been known to crystallize in polyrotaxanes with high macrocycle loadings,[3,4,21] even in PAN-rotaxa-60c20.[13]

The differential scanning calorimetry (DSC) thermogram for PAN-rotaxa-60c20 is shown in Figure 6. The T_g for the 60c20 is clearly observed at −64 °C. There is no indication of crystalline transitions for the 60c20 ($T_m \approx$ 55 °C). The PAN T_g also does not appear. While the calorimetric T_g of PAN is reported between 92 and 110 °C,[22] it is difficult to detect in the unthreaded PAN or the PAN-60c20 by DSC. Also shown in Figure 6 is the broad-component line width from the solid-state ^{1}H NMR line shape of PAN and PAN-rotaxa-60c20. For the latter, the line width remains 60 kHz until it reaches 90 °C, and then it begins to slowly decrease, thus marking the onset of motion in the PAN phase (the T_g). The solid-state ^{1}H NMR line width of unthreaded PAN behaves in a similar manner, except the decrease begins at a slightly higher temperature. For PAN, the line width is 63 kHz at room temperature and begins to decrease at 110 °C. Even though the polyrotaxane is phase separated, there is a small influence on the onset of the PAN T_g. This may be due to intermixing at the phase boundaries that must be present since the crowns are threaded onto the PAN backbones.

In Figure 6 it appears that solid-state NMR is a better method for detecting the glass transition in polyacrylonitrile (PAN) and PAN-containing materials. It should be noted that NMR, similar to other methods used for the detection of molecular motion, is certainly able to detect the drastic change in motional rates associated with a glass transition. However, information regarding the order of an arbitrary material transition needs to be established by calorimetric methods such as DSC.

The DSC and NMR data prove the 60c20 is phase-separated in the PAN matrix. The NMR data illustrate the large difference in mobility of the PAN versus the 60c20 phase. This mobility difference can be exploited to determine the domain sizes in this polyrotaxane through ^{1}H spin diffusion experiments.[19,23−29] The mobile-phase magnetization (i.e., 60c20 magnetization) was selected, allowed to diffuse for variable lengths of time, and then detected. Spin diffusion curves were generated and analyzed for details of the domain structure.[18,19]

The pulse sequence used to obtain the spin diffusion data is shown in Figure 2; the first step is selection of mobile-phase magnetization with a dipolar filter. Figure 7 shows the ^{1}H solid-state NMR spectrum of PAN-rotaxa-60c20 with and without selection. In the case where the dipolar filter has been applied, it is clear that the broad component of the ^{1}H line shape has been eliminated and the narrow component has been selected. The dipolar filter (see Figure 2) can be tuned to select more or less magnetization by adjusting the interpulse spacing (dipolar dephasing time) and the number of cycles. If the filter is too strong (interpulse spacings too large or too many cycles), magnetization from less mobile segments near the interface may not be selected. As discussed below, the filter parameters chosen resulted in very efficient selection of the entire 60c20-phase magnetization. To discern the chemical structure corresponding to the selected magnetization, a ^{13}C CP/MAS spectrum was acquired following the selection sequence. This is shown at the top of Figure 7 and clearly indicates the 60-crown-20 signal is retained and the PAN signal is suppressed. As the spin diffusion time was increased, ^{13}C NMR peaks around 30 and 120 ppm begin to reappear in the spectrum due to spin diffusion from the mobile crown units to the rigid PAN segments. After a spin diffusion time of about 100 ms the spectrum acquired was comparable to the ^{13}C CP/MAS spectrum, signifying the magnetization equilibrated in this time.

The spin diffusion data for the polyrotaxane at 24 and 80 °C are shown in Figure 8 along with spin diffusion data for a physical blend of PAN and 60c20. The room-temperature data reveal the magnetization has indeed equilibrated by 100 ms. For the polyrotaxane, numerical calculations of these data were conducted in order to extract details of the domain structure. For this purpose, a FORTRAN computer program provided by the Max Planck Institute for Polymer Research was used. The mathematical description of the data treatment as coded for these simulations has been described in detail by Schmidt-Rohr and Clauss.[18,19] Input variables for the simulation include the diffusion coefficients for the magnetization source (D_{crown}) and sink (D_{PAN}), the ratio of ^{1}H's in the two phases, and the dimensionality of the diffusion process. Guesses for the source and interface sizes are made until the computed spin diffusion curve matches the experimental data points. An interface is included by defining a spatially dependent diffusion coefficient (D_{inter}). For these simulations, it was assumed the D_{inter} varied linearly between the values given for the source and the sink.

There is much discussion in the literature about choosing appropriate spin diffusion coefficients. Values have been estimated based on theoretical considerations.[30−32] Experimentally determined values have been reported for systems in which the domain sizes were known from other techniques such as transmission electron microscopy (TEM) and small-angle X-ray scattering (SAXS).[19,33,34] Instead of creating polyrotaxanes suitable for calibrating diffusion coefficients, approximate values were obtained by comparison with experimentally determined values in other well-defined systems.

For the diffusion coefficient of the rigid PAN phase, an estimation procedure introduced by VanderHart[35] was used. (See the Appendix for a brief discussion of other methods for estimating rigid-phase spin diffusion coefficients.) It is based on comparing the relative proton densities of the sample with unknown diffusion constant with a reference sample in which the diffusion coefficient is known. The reference sample chosen is a rigid diblock copolymer of poly(methyl methacrylate) and polystyrene (PMMA-PS) in which the diffusion coefficient was determined experimentally.[19] These samples had well-characterized domain sizes by SAXS and TEM. Spin-diffusion measurements were conducted (selection was based on chemical structure) and the spin diffusion coefficients defined so that the NMR long periods correlated to those determined by TEM and SAXS. The $D_{\text{PMMA−PS}}$ thus determined was 0.8 ± 0.2 nm^2/ms. The D_{PAN} was estimated according to the following relation:

$$D_{\text{PAN}}/D_{\text{PMMA−PS}} = (\rho^{\text{H}}_{\text{PAN}}/\rho^{\text{H}}_{\text{PMMA−PS}})^{1/3} \qquad (1)$$

The $D_{\text{PMMA−PS}}$ and $\rho^{\text{H}}_{\text{PMMA−PS}}$ were taken directly from the literature.[19] The $\rho^{\text{H}}_{\text{PAN}}$ was calculated from the material density (1.137 g/cm^3)[36] and the ^{1}H fraction (0.057). Using eq 1, the D_{PAN} was estimated as 0.72 nm^2/ms.

For the diffusion coefficient of the mobile 60-crown-20 phase, a calibration curve for mobile polymers recently established by Mellinger was used.[34] The curve was developed by conducting ^{1}H spin diffusion measurements on a series of diblock copolymers in which the long periods were known from SAXS. Most of the reference materials were diblocks of polystyrene (PS) and polyisoprene (PI); around room temperature, the PS block is rigid and the PI block is mobile. One of the materials contained a mobile poly(ethylene oxide) phase, which is particularly relevant because of the structural similarities with 60-crown-20. The spin diffusion coefficients of the mobile phases were computed from the spin diffusion data and the known long periods. The following calibration curve was constructed and correlates spin diffusion coefficient to inverse T_2:

$$D_{\text{mobile}} = [4.55 \times 10^{-5}(\Delta\nu_{1/2})^{1.5} + 0.007]\ \text{nm}^2/\text{ms} \qquad 0 < \Delta\nu_{1/2} \le 300\ \text{Hz} \quad (2)$$

where $\Delta\nu_{1/2}$ is the full width at half-maximum of the ^{1}H line width, or $1/\pi T_2$. The ^{1}H line width determined directly from an NMR spectrum is the inverse T_2* and for mobile phases may be complicated by chemical shift dispersion. Thus, the T_2 was measured directly using a Hahn echo sequence. By placing the Hahn echo se-

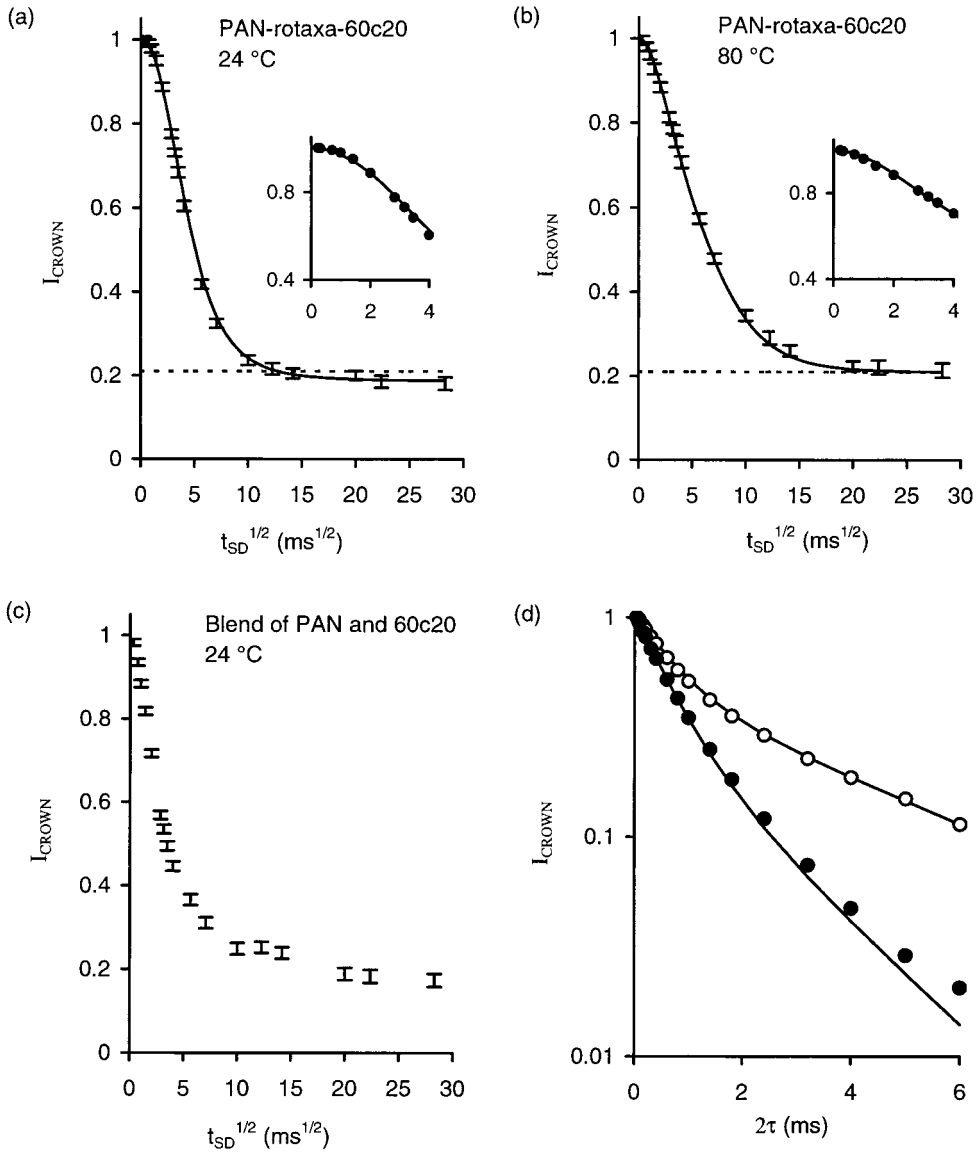

Figure 8. Spin diffusion data for PAN-rotaxa-60c20 (a, b) and a solution-blended physical mixture of PAN and 60c20 (c). Simulations are shown for the PAN-rotaxa-60c20 data. The insets clearly illustrate that the source magnetization does not decrease linearly for short $t_{SD}^{1/2}$'s, thereby signifying the presence of a mixed interface. The dashed horizontal lines on these plots represent the theoretical end value for the spin diffusion process, computed from the ratio of 60c20 to PAN protons. Hahn echo decay curves and fits for the mobile component of PAN-rotaxa-60c20 (d): (●) 24 °C, (○) 80 °C.

quence after the dipolar filter, the T_2 of the same mobile phase selected in the spin diffusion experiment was measured (see Figure 2b). Hahn echo decay curves for the PAN-rotaxa-60c20 are shown in Figure 8 for T = 24 and 80 °C. As expected, the decay is slower at the higher temperature (i.e., longer T_2) due to a general reduction in the dipolar couplings as the 60c20 becomes more mobile.

Neither echo decay curve could be adequately analyzed as a single exponential. They were fitted with a biexponential from which two T_2's and the respective mass fractions of the two components were extracted. At each temperature, a weighted average T_2 was computed and used to determine the diffusion coefficient for the mobile crown phase. It is likely that a distribution of T_2's more complicated than the assumed bimodal exists; this procedure was merely used to obtain an average T_2 value from which a diffusion coefficient (D_{mobile}) for the selected magnetization could be calculated. The fact that the mobile-phase T_2 decay could not be fit with a single exponential reveals a dynamic heterogeneity that we attribute to interaction between the mobile crowns and the rigid PAN backbone. The existence of rigid 60c20 segments within PAN-rotaxa-60c20 has been proven by 2D WISE NMR (see Figure 5). These rigid 60c20 segments can be considered as those that approach and enter the interfacial area with the rigid PAN phase, while crown segments with the highest mobilities can be considered as the center of the 60c20 domains. Hence, a mobility gradient exists within the 60c20 phase.

At 80 °C an average mobile-phase T_2 of 2.2 ms was measured from which an effective line width of 140 Hz was computed. According to eq 2, this corresponds to a diffusion coefficient, $D_{crown}^{80\,°C}$, of 0.08 nm^2/ms. The average mobile-phase T_2 at 24 °C is 1 ms, which corresponds to an effective line width of 320 Hz. This value falls just outside the range of the Mellinger calibration curve shown as eq 2. Mellinger has also prepared a calibration curve for the region $300 < \Delta\nu_{1/2} < 1100$ Hz.[34] Using this calibration, the computed diffusion coefficient was the same as that calculated using eq 2 since the $\Delta\nu_{1/2}$ used

Table 1. Domain Sizes in PAN-rotaxa-60C20

	24 °C	80 °C
d_{crown} (nm)	6	8
d_{inter} (nm)	4	2
d_{PAN} (nm)	10	10
long period (nm) = $d_{crown} + 2d_{inter} + d_{PAN}$	24 ± 2	22 ± 2
SAXS correlation length (nm)	19	

for the calculations occurs at the intersection of the two curves. The diffusion coefficient at 24 °C, $D_{crown}^{24\ °C}$, was determined to be 0.26 nm^2/ms by both calibration curves.

From the solution-state ^{1}H NMR spectrum, the ratio of protons (60c20/PAN) was calculated to be 0.21. Since the initially selected magnetization is redistributed via spin diffusion, the end value in the normalized spin diffusion plots should reach 0.21. This value is represented on the PAN-rotaxa-60c20 spin diffusion plots of Figure 8 as horizontal dashed lines.

The dimensionality can be 1 (lamellae), 2 (cylinders), or 3 (spheres). The mass fraction of the minor phase is 15% for the 60c20 in PAN-rotaxa-60c20. With diblock copolymers, this value falls within the morphological transition region of spheres to cylinders for the minor component fraction (spheres, 0−0.2; cylinders, 0.15−0.4).[37] While no polyrotaxane has been shown to exhibit microphase-separated morphologies analogous to diblocks, it is conceivable that they could, given the fact that threaded macrocycles can have uniform sizes. Thus, the choice of dimensionality for the spin diffusion simulation is indeed a point of uncertainty in the computed domain sizes. While a dimensionality of 2 was used to calculate the domain sizes reported here, simulations were done with dimensionalities of both 2 and 3; the error in the reported NMR long periods reflects these two values for a given set of spin diffusion data.

The spin diffusion simulation results are shown in Table 1. The presence of a mixed interface in the PAN-rotaxa-60c20 is indicated by the shape of the spin diffusion curves at small t_{SD}'s: following selection, the magnetization does not immediately decrease with $t_{SD}^{1/2}$ in a linear fashion. Thus, there is some lag in the diffusion process, implying the magnetization does not immediately contact the phase characterized by the largest diffusion constant (i.e., D_{PAN}). This is completely expected given the fact that 60-crown-20 is threaded onto the PAN backbone; a mixed interface is required based on the entangled rotaxane structure. In contrast, the spin diffusion curve for the physical blend (see Figure 8) linearly decreases at small t_{SD} without a lag, thus indicating a much sharper interface. Since the macrocycles are not threaded in this sample, more complete phase separation is possible. Evidence for this was already provided in the ^{13}C CP/MAS spectrum of the blend (see Figure 4), which is basically a superposition of the ^{13}C spectra for the free 60-crown-20 and the unthreaded PAN. A simulated curve for the blend is not shown for the following reasons: (1) since the morphology is so dependent on sample preparation, computed domain sizes are meaningful for the sample and not the material, and (2) since the ^{13}C CP/MAS spectrum revealed the crown exists as both crystalline and amorphous material, three phases with three spin diffusion constants must be considered, which is beyond the scope of this report. The simulated curve for the polyrotaxane at 24 °C falls below the dashed horizontal line representing the theoretical end value computed from the 60c20/PAN ^{1}H fractions. Thus, some of the crown was not selected by the dipolar filter. The rigid part of the crown phase suppressed by the filter is attributed to interfacial 60c20. This rigid fraction was also detected by the 2D WISE experiment as described above.

Upon heating the PAN-rotaxa-60c20 to 80 °C, changes in the domain structure include a decrease in the interface and a complementary increase in the 60c20 domain size. Note the end value for the spin diffusion curve is the same as the theoretical end value marked by the dashed line. Thus, as opposed to the selection at 24 °C, the selection at 80 °C appears to be complete, reflecting the sufficiently high mobility (for this dipolar filter) of the interfacial segments of the crown. The data also reflect the tendency of the PAN-60c20 system to phase separate instead of mix with increasing temperature. This tendency toward phase separation is consistent with the DSC and NMR data presented here for the solution-blended physical mixture; despite the potential for association between the crown ether oxygen and the acidic proton α to the cyano group in PAN,[38] the blend phase separated with a relatively nondiffuse interface.

Small-angle X-ray scattering of the PAN-rotaxa-60c20 revealed no peaks. This is consistent with the absence of periodicity in the spatial distribution of the phase-separated 60c20 domains within the PAN matrix. This is also an indication that domains are not uniform in size. From the scattering curve, the correlation length of electron density fluctuation was computed following a Debye−Bueche treatment which assumes a random two-phase structure characterized by a single-exponential correlation function.[39] A plot of $I(q)^{-1/2}$ versus q^2 gave a straight line for a q range of 0.11−0.19 nm^{-1}. The correlation length was computed from the slope of this plot[40] to be 19 nm. As shown in Table 1, this value compares reasonably well with the NMR long period determined from the spin diffusion measurements. In fact, the actual domain sizes may be smaller than those listed in Table 1: Simulations that consider a distribution in domain sizes or separation have been shown to provide average domain sizes smaller than those computed from random two-phase/two-domain models such as that used here.[41]

The typical smallest diameter of the 60-crown-20 domains was determined from the spin diffusion experiments to be 6 nm at 24 °C and 8 nm at 80 °C (see Table 1). A physical picture of what this domain size might mean can be gained by considering the size and shape of the 60-crown-20 molecule in the solid state. To do this, it is instructive to refer to the reported crystal structure of 30-crown-10.[42] Anhydrous 30-crown-10 crystallizes in a flat, extended form consisting of two tight loops connected by two parallel linear segments in which all the C−C bonds are in anti conformations. Each of the two end loops is formed by two ethylene oxide units in which the C−C bonds are in gauche conformations. The length of this molecular arrangement for 30-crown-10 is 1.36 nm. If we assume the same extended conformation for 60-crown-20, in which each of both end loops is comprised of two ethylene oxide units, a length of 3.6 nm is computed (see Figure 1). As noted for 30-crown-10, this fully extended conformation has no cavity, and 3.6 nm is therefore too large for an extended 60-crown-20 molecule that is threaded by a polymer chain. Thus, it provides an upper bound for the distance that a 60-

crown-20 segment can be from a PAN segment to which it is threaded. If the domain shapes were regular with smooth surfaces, the maximum distance across a 60c20 domain would be 7.2 nm, or twice the maximum distance from the center of a domain to a PAN segment at the interface. Indeed, the domain size should be smaller than this since threading necessarily decreases the extension of the 60-crown-20 molecules; the PAN backbone is accommodated in a cavity that can only be created if some of the C−C bonds exist in gauche conformations, which causes a decrease from full extension. The experimentally determined 60c20 domain sizes of 6−8 nm compare reasonably well with the theoretical 7.2 nm cross-domain distance, thus suggesting the 60c20 domains consist of an average of two 60-crown-20 molecules across their smallest diameters. However, 7.2 nm was presented as an upper bound. In fact, the actual domain sizes may be smaller than 6−8 nm (vide supra). On the other hand, the 60-crown-20 used to prepare the PAN-rotaxa-60c20 may contain some fraction of larger macrocycles that would increase the average domain size.[14] Thus, a typical 60c20 domain in PAN-rotaxa-60c20 consists of an average of two "60-crown-20" molecules across its smallest diameter. Other polyrotaxanes are being examined to determine whether domain sizes are a simple function of macrocycle size.

It is interesting to compare these results with those found for polymers containing unthreaded low-molecular-weight, low-T_g diluents. For example, NMR studies on polycarbonate containing at least 10% phosphate ester diluent revealed two populations for the unthreaded plasticizer: a less mobile fraction consisting of isolated plasticizer molecules and a more mobile fraction due to clusters of two plasticizer molecules.[43−46] The appearance of the two-molecule clusters was accompanied by enhanced mobility for the associated backbone segments and diluent molecules, resulting in a bulk plasticization effect. In a mixed PAN/60c20 system, the low-T_g component is not a diluent but an additive that phase separates. Since complete phase separation is prevented in the PAN-rotaxa-60c20, some degree of interaction between 60c20 segments and PAN segments is ensured. It is not yet clear what effect such interactions have on bulk mechanical properties of polyrotaxanes.

Conclusions

Poly[(acrylonitrile)-rotaxa-(60-crown-20)] was studied with solid-state NMR techniques to elucidate structure and mobility in this polyrotaxane. Unthreaded 60-crown-20 contained both amorphous and crystalline regions, with solid-state NMR spectra very similar to oligomeric poly(ethylene oxide). When threaded onto the linear polymer ($x/n = 0.01$, mass fraction = 15%), the crown was found to be phase-separated, predominantly amorphous, and highly mobile. The PAN T_g was undetectable by DSC but clearly seen with ^{1}H solid-state NMR. While it is well-known that solid-state ^{1}H NMR can be used to detect glass transitions, these results reinforce the use of the method for polymers that do not show a clear transition in a DSC trace.

Even though the 60c20 is phase separated in the polyrotaxane, the PAN T_g (90 °C) was slightly reduced compared to that of the unthreaded PAN backbone (110 °C). This was attributed to the intermixing that must be present at the phase boundaries due to the rotaxane structure. Evidence for these mixed interfaces was seen in the spin diffusion data, which also indicated the physical blend tended toward a strongly segregated morphology. Polyrotaxanation can thus be used for modifying polymer properties by forcing incompatible components to be mixed, at least within an interfacial region composed of the macrocycle segments that loop around the host backbone. Because of this construction, the polymer microphase structure should also be thermally stable, at least up to the glass transition of the rigid phase. Since the incompatible 60c20 and PAN segments are not linked to each other via covalent bonds, the 60c20 is able to maintain a high degree of mobility in this polyrotaxane, a characteristic which may have important consequences for bulk physical properties of polyrotaxanes in general.

Table 2. Other Methods of Estimating Rigid-Phase Spin Diffusion Coefficients and Resultant Domain Sizes in PAN-rotaxa-60c20

equation		D_{PAN} (nm^2/ms)	d_{crown} (nm)	d_{inter} (nm)	d_{PAN} (nm)
$D_R = k\langle r^2\rangle\Delta\nu_{1/2}$	(A1)	0.48	5	4	8.8
$D_R = D_{ref}\dfrac{\langle r^2\rangle_R}{\langle r^2\rangle_{ref}}\dfrac{[\Delta\nu_{1/2}]_R}{[\Delta\nu_{1/2}]_{ref}}$	(A2)	1.3	6.6	4.6	10.8

Acknowledgment. Support from the National Science Foundation (CMS-9412294, DMR-9502246, and DMR-9706909), the Molecular Design Institute, and the Office of Naval Research (Chemistry Division) is gratefully acknowledged. Access to NMR instrumentation through the Georgia Tech NMR Center has been made possible by an NSF DMR instrumentation grant (DMR-9503936). We also thank the following individuals: Jason Hunt for the preparation of the 60-crown-20, Ralph Ulrich of the Max-Planck-Institut für Polymerforschung (MPI-P) for the corrected SAXS data, and Felix Mellinger of the MPI-P for valuable discussions concerning spin diffusion.

Appendix. Estimation of Rigid-Phase Spin Diffusion Coefficient

In addition to the VanderHart procedure, two other methods were used to estimate the rigid-phase spin diffusion coefficient (D_R). The relevant equations are shown in Table 2 along with the calculated spin diffusion coefficients (D_{PAN}) and the resulting domain sizes determined from simulated spin diffusion curves. In these equations, $\Delta\nu_{1/2}$ is the full width at half-height of the ^{1}H solid-state spectrum, and r is the average distance between nearest protons. For PAN in the polyrotaxane, the measured $\Delta\nu_{1/2}$ was 60 kHz and r was taken to be 0.25 nm, a value used for other vinyl polymers.[18]

Equation A1 was derived from theoretical considerations and is commonly used since $\Delta\nu_{1/2}$ can be directly measured and the average distance between nearest protons can be determined from the structure, X-ray, or density data.[31,43] For Gaussian line shapes, $k = 1/12\text{-}(\pi/2 \ln 2)^{1/2} = 0.125$.[32] Using this equation, D_{PAN} is calculated as 0.48 nm^2/ms, which is less than the value estimated by the VanderHart procedure. Dividing eq A1 by the same expression for a reference material with known spin diffusion coefficient provides eq A2.[18,32] The reference material used here is a PMMA-PS diblock copolymer[19] with $D_{ref} = 0.8 \pm 0.2$ nm^2/ms, $[\Delta\nu_{1/2}]_{ref} =$ 38 kHz, and $\langle r^2\rangle_{ref} = 0.0625$ nm^2. Using this scaling

relation, D_{PAN} is calculated as 1.3 nm^2/ms, which is greater than the value estimated by the VanderHart procedure.

The values shown in Table 2 for the domain characteristics were determined by fitting the spin diffusion data of Figure 8 (24 °C); the only difference was the D_{PAN} value used in the simulation. Thus, the domain sizes may be compared with the domain sizes reported in Table 1 (24 °C) to assess the sensitivity of the simulations on the D_{PAN} value. As shown in Table 2, changing D_{PAN} from 0.48 to 1.3 nm^2/ms returns d_{crown} values from 5 to 6.6 nm. The difference in the computed domain sizes is not significant. This relatively weak dependence of the computed domain sizes on the spin diffusion coefficients has been noted before and attributed to the coefficients entering the analysis as the square root of an effective diffusion coefficient.[35] Using an estimation method based on relative proton densities, an intermediate D_{PAN}, 0.72 nm^2/ms, was calculated and used for the simulated spin diffusion curves shown in Figure 8.

References and Notes

(1) Gibson, H. W.; Bheda, M. C.; Engen, P. T. *Prog. Polym. Sci.* **1994**, *19*, 843.
(2) Gibson, H. W. In *Large Ring Molecules;* Semlyen, J. A., Ed.; J. Wiley and Sons: New York, 1996; Chapter 6.
(3) Gibson, H. W.; Liu, S.; Gong, C.; Joseph, E. *Macromolecules* **1997**, *30*, 3711.
(4) Gibson, H. W.; Liu, S.; Lecavalier, P.; Wu, C.; Shen, Y. X. *J. Am. Chem. Soc.* **1995**, *117*, 852.
(5) Gong, C.; Subramaniam, C.; Ji, Q.; Gibson, H. W. *Macromolecules* **1997**, *31*, 1814.
(6) Lipatova, T. E.; Kosyanchuk, L. F.; Shilov, V. V. *J. Macromol. Sci., Chem.* **1985**, *A22*, 361.
(7) Gibson, H. W.; Marand, H. *Adv. Mater.* **1993**, *5*, 11.
(8) Marand, H.; Prasad, A.; Wu, C.; Bheda, M. C.; Gibson, H. W. *Polym. Prepr. (Am. Chem. Soc., Div. Polym. Chem.)* **1991**, *32* (3), 639.
(9) Shen, Y. X.; Xie, D.; Gibson, H. W. *J. Am. Chem. Soc.* **1994**, *116*, 537.
(10) Loveday, D.; Wilkes, G. L.; Bheda, M. C.; Shen, Y. X.; Gibson, H. W. *J. M. S.-Pure Appl. Chem.* **1995**, *A32*, 1.
(11) Hunt, J. P.; Nagapudi, K.; Beckham, H. W. *Polym. Prepr. (Am. Chem. Soc., Div. Polym. Chem.)* **1997**, *38* (1), 84.
(12) Nagapudi, K.; Hunt, J. P.; Shepherd, C.; Baker, J. E.; Beckham, H. W. *Macromol. Chem. Phys.,* in press.
(13) Gibson, H. W.; Engen, P. T. *New J. Chem.* **1993**, *17*, 723.
(14) Gibson, H. W.; Bheda, M. C.; Engen, P.; Shen, Y. X.; Sze, J.; Zhang, H.; Gibson, M. D.; Delaviz, Y.; Lee, S.-H.; Liu, S.; Wang, L.; Nagvekar, D.; Rancourt, J.; Taylor, L. T. *J. Org. Chem.* **1994**, *59*, 2186. Recent high-resolution GPC and MS studies have revealed that the larger (>30c10) crown ethers prepared by this method consist of a distribution of ring sizes up to several times the targeted values.
(15) Earlier reported as $x/n = 0.2$: Nagapudi, K.; Gibson, H. W.; Beckham, H. W. *Polym. Mater. Sci. Eng. (Prepr. Am. Chem. Soc., Div. Polym. Mater. Sci. Eng.)* **1998**, *78*, 130.
(16) Dixon, W. T. *J. Chem. Phys.* **1982**, *77*, 1800.
(17) Schmidt-Rohr, K.; Clauss, J.; Spiess, H. W. *Macromolecules* **1992**, *25*, 3273.
(18) Schmidt-Rohr, K.; Spiess, H. W. *Multidimensional Solid-State NMR and Polymers*; Academic: New York, 1994.
(19) Clauss, J.; Schmidt-Rohr, K.; Spiess, H. W. *Acta Polym.* **1993**, *44*, 1.
(20) Dechter, J. J. *J. Polym. Sci., Polym. Lett.* **1985**, *23*, 261.
(21) Shen, Y. X.; Gibson, H. W. *Macromolecules* **1992**, *25*, 2058.
(22) Howard, W. H. *J. Appl. Polym. Sci.* **1961**, *5*, 303.
(23) Goldman, M.; Shen, L. *Phys. Rev.* **1966**, *144*, 321.
(24) Assink, R. A. *Macromolecules* **1978**, *11*, 1233.
(25) Ishida, M.; Yoshinaga, K.; Horii, F. *Macromolecules* **1996**, *29*, 8824.
(26) Li, K.-L.; Jones, A.; Inglefield, P. T.; English, A. D. *Macromolecules* **1989**, *22*, 4198.
(27) Havens, J. R.; VanderHart, D. L. *Macromolecules* **1985**, *18*, 1663.
(28) Cheung, T. T. P. *Phys. Rev. B* **1981**, *23*, 1404.
(29) Packer, K. J.; Pope, J. M.; Yeung, R. R.; Cudby, M. E. A. *J. Polym. Sci., Polym. Phys.* **1984**, *22*, 589.
(30) Abragam, A. *Principles of Nuclear Magnetism*; Clarendon: Oxford, 1961.
(31) Cheung, T. T. P.; Gerstein, B. C. *J. Appl. Phys.* **1981**, *52*, 5517.
(32) Demco, D. E.; Johansson, A.; Tegenfeldt, J. *Solid State Nucl. Magn. Reson.* **1995**, *4*, 13.
(33) Kimura, T.; Neki, K.; Tamura, N.; Horii, F.; Nakagawa, M.; Odani, H. *Polymer* **1992**, *33*, 493.
(34) Mellinger, F. Ph.D. Dissertation, Johannes Gutenberg-Universität, 1998.
(35) VanderHart, D. L.; McFadden, G. B. *Solid State Nucl. Magn. Reson.* **1996**, *7*, 45.
(36) Hinrichsen, G.; Orth, H. *Kolloid Z. Z. Polym.* **1971**, *247*, 844.
(37) Goodman, I., Ed. *Developments in Block Copolymers-1*; Applied Science Publishers: New York, 1982.
(38) Mosier-Boss, P. A.; Popov, A. I. *J. Am. Chem. Soc.* **1985**, *107*, 6168.
(39) Debye, P.; Bueche, A. M. *J. Appl. Phys.* **1949**, *20*, 518.
(40) VanderHart, D. L.; Campbell, G. C.; Briber, R. M. *Macromolecules* **1992**, *25*, 4734.
(41) Cheung, T. T. P. *Appl. Spectrosc.* **1997**, *51*, 1703.
(42) Bheda, M. C.; Merola, J. S.; Woodward, W. A.; Vasudevan, V. J.; Gibson, H. W. *J. Org. Chem.* **1994**, *59*, 1694.
(43) Liu, Y.; Inglefield, P. T.; Jones, A. A.; Kambour, R. *Magn. Reson. Chem.* **1994**, *32*, S18.
(44) Liu, Y.; Roy, A. K.; Jones, A. A.; Inglefield, P. T.; Ogden, P. *Macromolecules* **1990**, *23*, 968.
(45) Liu, Y.; Turnbull, M. M.; Jones, A. A.; Inglefield, P. T.; Kambour, R. P. *Solid State Nucl. Magn. Reson.* **1993**, *2*, 289.
(46) Jones, A. A.; Inglefield, P. T.; Liu, Y.; Roy, A. K.; Cauley, B. J. *J. Non-Cryst. Solids* **1991**, *131*−*133*, 556.

MA9813082